

Effect of Predators of Juvenile Rodents on the Spread of the Hantavirus Epidemic

G. Camelo-Neto^a, Ana T.C. Silva^{a,b}, L. Giuggioli^a,
V.M. Kenkre^a

^a*Consortium of the Americas for Interdisciplinary Science and Department of Physics, University of New Mexico, Albuquerque, NM 87131, USA.*

^b*Departamento de Física, Universidade Estadual de Feira de Santana, Feira de Santana, BA 44031-460, Brazil*

Abstract

Effects of predators of juvenile mice on the spread of the Hantavirus are analyzed in the context of a recently proposed model. Two critical values of the predation probability are identified. When the smaller of them is exceeded, the hantavirus infection vanishes without extinguishing the mice population. When the larger is exceeded, the entire mice population vanishes. These results suggest the possibility of control of the spread of the epidemic by introducing predators in areas of mice colonies in a suitable way so that such control does not kill all the mice but lowers the epidemic spread.

Key words: Hantavirus epidemic, predator, control of spread

1 Introduction and the Model

The Hantavirus epidemic (Yates et al., 2002; Mills et al., 1999), known to be spread by the movement of, and virus transmission between, mice, has received a lot of mathematical attention in the last few years (Abramson and Kenkre, 2002; Aguirre et al., 2002; Abramson et al., 2003; Kenkre, 2003; Buceta et al., 2004; Escudero et al., 2004; Kenkre, 2005). Recently, we proposed a model (Kenkre et al.,

Email addresses: gustavo@phys.unm.edu (G. Camelo-Neto), tereza@uefs.br (Ana T.C. Silva), giuggioli@unm.edu (L. Giuggioli), kenkre@unm.edu (V.M. Kenkre).

2005) characterized by two types of mice: itinerant juvenile mice known technically in the biological literature as subadults that roam in their attempts to find their own home ranges until they find a suitable place, at which time they turn into adult mice; and the relatively less mobile adult mice that restrict their movements within their own home ranges. Given the two extreme types of movement (freely diffusing and static) that the juveniles and the adult perform in the field, the model has been termed the *liquid-solid* (LS) model. An analysis of the LS model has been provided (Kenkre et al., 2005) on the basis of mean field calculations as well as computer simulations that incorporate spatial features. To simplify the analysis it was assumed in that work that the juvenile mice do not die; that they cease to exist only when they grow into adult mice on finding a suitable site to call their own home range. While it allows a quicker insight into the consequences of the main aspects of the model, that assumption is surely not realistic in many situations. The itinerant juvenile mice might meet with predators in the open field and be killed by them. The purpose of the present study is to explore the effects of the predator-induced attrition in the juvenile population.

Our analysis below shows that two transitions occur as a direct consequence of this realistic feature. The infected phase vanishes for sufficiently large predation ‘pressure’ whatever the value of the other parameters. In particular, this happens even in the presence of unlimited environment resources (e.g., food). The second transition is the appearance of a bifurcation when the rate at which the juveniles are converted into adults is varied. A population is sustained by the environment only if juveniles grow into adults fast enough to avoid being killed by the predators.

As explained in our earlier analysis (Kenkre et al., 2005), the LS model may be represented at the *kinetic* level by

$$\begin{aligned}
\frac{\partial B_i(x, t)}{\partial t} &= -c_B B_i - \frac{B_i(A + B)}{K(x, t)} + aB_s(A_i + B_i) + D\nabla^2 B_i - G(x)B_i, \\
\frac{\partial B_s(x, t)}{\partial t} &= bA - c_B B_s - \frac{B_s(A + B)}{K(x, t)} - aB_s(A_i + B_i) + D\nabla^2 B_s - G(x)B_s, \\
\frac{\partial A_i(x, t)}{\partial t} &= -cA_i - \frac{A_i(A + B)}{K(x, t)} + aA_s B_i + G(x)B_i, \\
\frac{\partial A_s(x, t)}{\partial t} &= -cA_s - \frac{A_s(A + B)}{K(x, t)} - aA_s B_i + G(x)B_s,
\end{aligned} \tag{1}$$

where A and B (without suffixes) denote the total densities of the adult and juvenile mice respectively, the suffixes i and s represent infected and susceptible states of the mice, and the last terms in each equation describe the settling down of the juveniles into their own homes, accompanied by their conversion into (static) adults. The rate of such conversion, $G(x)$, is non-zero only if

the spatial coordinate of the mouse, x , lies in regions that the juveniles find suitable as their home ranges. An extreme way of representing the confinement of the adults to their home ranges, used in this LS model, is to take the adults to be immobile. Because we use such a representation for simplicity (Kenkre et al., 2005), there are no spatial derivatives in the equations for the adults. The other parameters of the model are as follows: b is the birth rate of the juveniles, c is the death rate of the adults, a is the infection parameter, D is the juvenile diffusion constant, and K is the environment parameter that, for the sake of simplicity in this analysis, we consider to be independent of time and space. Our particular focus is on the introduction of c_B , the death rate of the juveniles. That parameter, assumed zero for simplicity in our earlier analysis, is here controlled by the presence of the predators.

2 Simulation analysis

Our analysis here is at the configuration master equation approach rather than at the kinetic level implied by (1). For this purpose we carry out simulations on a $L \times L$ square lattice with each site of the lattice corresponding to a small region in the landscape. We use moderately large lattices (with a total of 2^{14} sites) and discrete time evolution. At each time step, the juveniles may move but the adults not, the probability for the diffusive (random walk) motion being 0.125 for any of the 8 directions of the square lattice. Our time step is scaled in this manner to the diffusion constant. An adult, infected or susceptible, gives birth to a susceptible juvenile with probability P_b . An adult dies by aging with probability P_c . When two or more mice meet at a site, they compete and one may die with probability $1 - P_K$. If a susceptible mouse occupies the same site as an infected mouse, the former has probability P_a of getting infected in the next time step. A juvenile dies because of predation with probability P_p and, if it is at a site without an adult, grows up settling in that site with probability P_g . Corresponding to the kinetic level parameters of equations (1), b , c , c_B , g , a , and K , we have the respective probabilities in the simulation description, P_b , P_c , P_p , P_g , P_a , and P_K . Our focus in the present study is on P_p .

Our extensive computer simulations with attention on effects that are qualitatively different from the case of vanishing P_p analyzed earlier, show a clear existence of separate infected, non-infected and no-life phases. In Fig. 1 the steady state values of the infected and the total mice populations are plotted as functions of the ratio of the predation probability P_p to the adult death probability P_c . Sufficiently large values of the ratio make the total mice population disappear because the predators kill all the juveniles and the adults die their natural deaths. This is trivially expected. However, an important finding in Fig. 1 is related to the existence of the middle region of the x -axis, lying

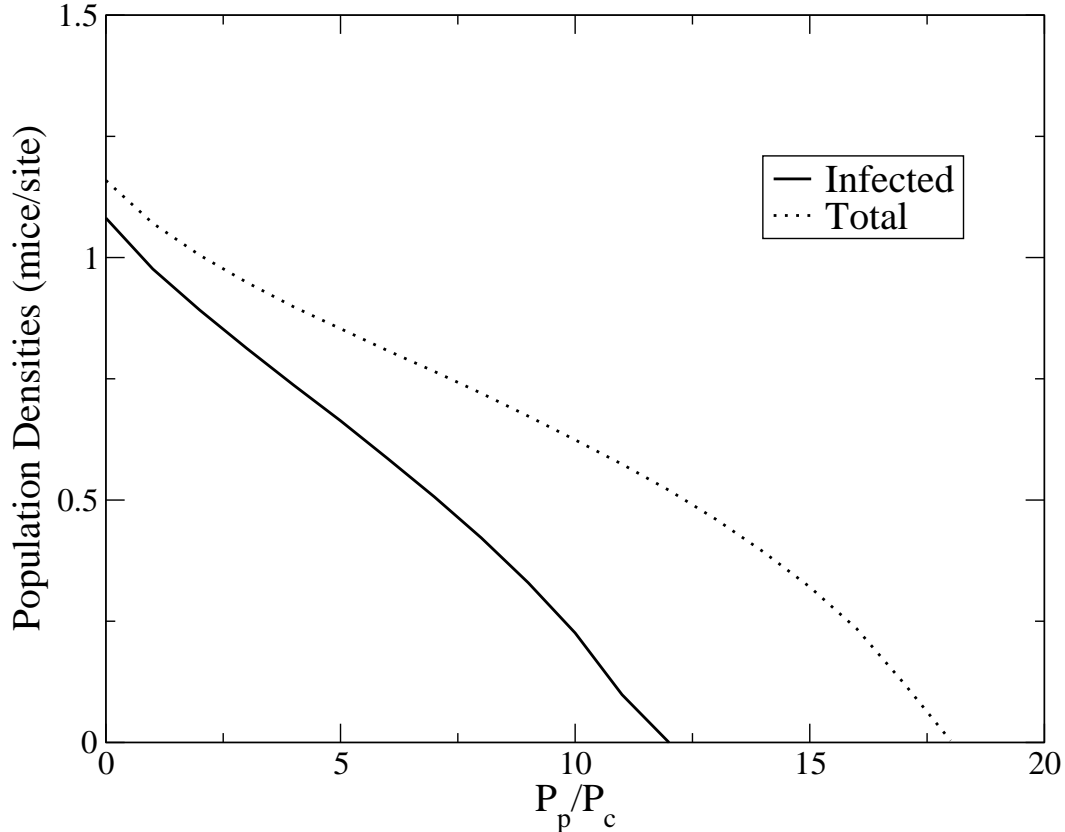


Fig. 1. Steady state densities of the infected and susceptible populations versus P_p/P_c , the probability of the predation-induced death of the juveniles divided by the death probability of the adults. Other parameters are $P_c = 0.01$, $P_b = 0.02$, $P_g = 0.6$, $P_a = 0.3$ and $P_K = 0.98$.

between the values of 12 and 18 for the particular parameter values chosen, where the infected population has died out but the total population has not. The fact that predation thus buffers the transmission of infection nontrivially, and may be thus used to eliminate it without killing off all mice, is worthwhile to note.

One characteristic of the model (1), for the case $P_p = 0$, is the fact that, as competition decreases, eventually an infected phase appears (if $P_b > P_c$ and irrespective of P_a and P_g). In other words, as the environment accommodates a larger population, infection will always appear beyond a certain value of P_K . This does not necessarily happen when $P_p \neq 0$. The $P_p - P_K$ phase plot in Fig. 2 makes this clear. For a certain range of P_p values, the system remains susceptible for any value of P_K . An increase in food availability has only the effect of increasing the susceptible populations. Thus, the introduction of an appropriate number of predators in an infected area may completely eliminate the infection. It is the presence of clusters of adults in the landscape that is responsible for this effect. If $P_p = 0$, a juvenile cannot find a free site where to settle inside a cluster and is forced to roam for a long period of time, increasing

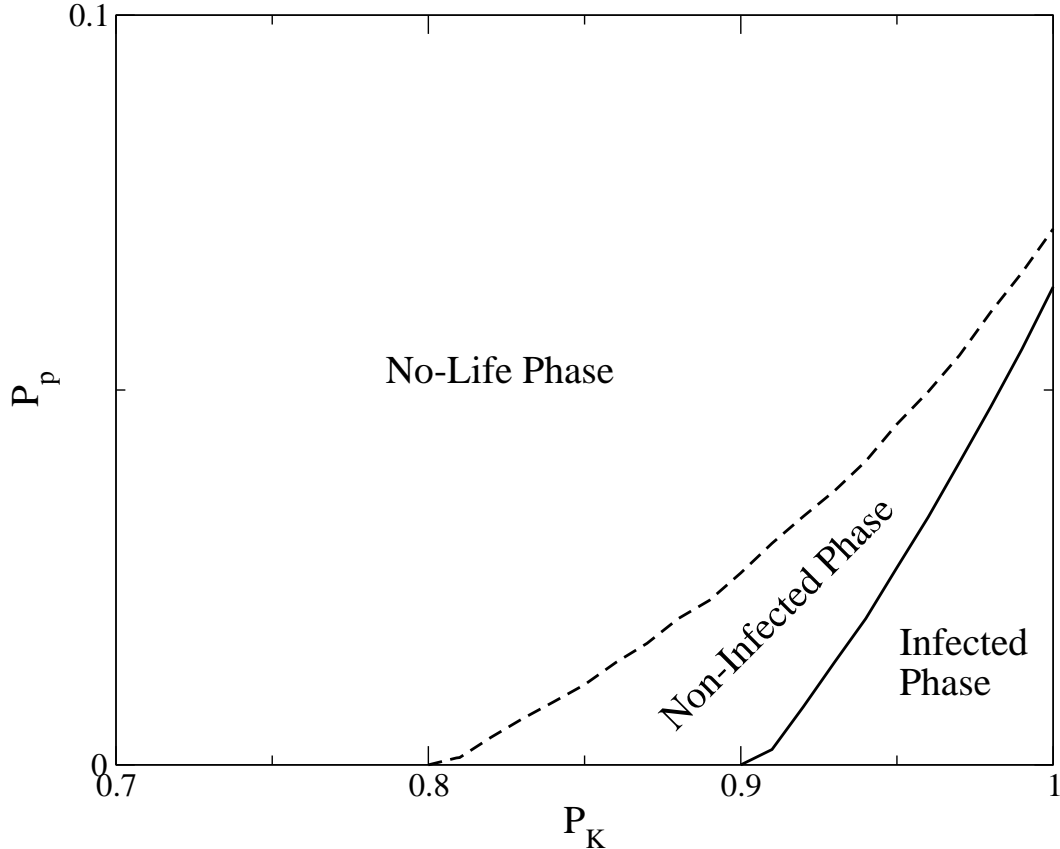


Fig. 2. $P_p - P_K$ Phase plot showing system behavior in various regions of the predation probability P_p and the environment-controlled survival probability P_K . There are clear regions where there is an infected phase, a non-infected phase, and a phase in which no mice are living. This shows that if the predator ‘pressure’ is in the right level, infection can be eliminated without killing all mice. The other parameters are: $P_c = 0.01$, $P_b = 0.02$, $P_g = 0.1$ and $P_a = 0.3$.

the chance of being infected and transmitting the infection. On the other hand, when $P_p > 0$, the adult clusters reduce the transmission of infection because the juveniles are subject to predation as long as they roam in the landscape and do not settle into a home range. A susceptible population may thus exist without infection. Since any increment in the environmental resources reduces competition and increases the cluster size, if P_p is sufficiently large, an increase of P_K maintains the entire population without infection.

The dependence of this infection-free regime on the other parameters is studied in Fig. 3 where the $P_p - P_g$ phase plot is shown. In particular, we see how the window of P_p values, where no infection appears, gets larger as P_g increases. Bigger values of P_g reduces the effect of predation by converting the juveniles more rapidly into adults. In order to reach the condition with zero steady state population, a larger P_p value is necessary. From Fig. 3 we also see a different qualitative characteristic of the steady state populations depending on whether P_p is zero or larger than zero. For a given $P_p > 0$, the system may

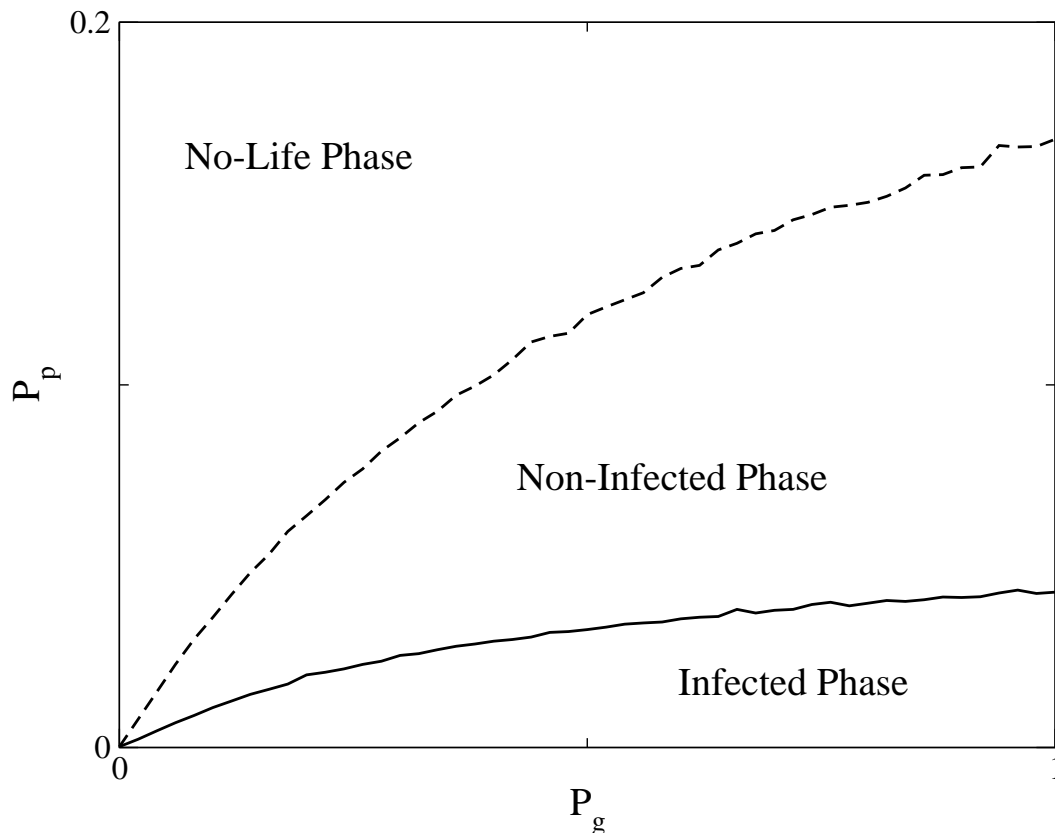


Fig. 3. $P_p - P_g$ Phase plot showing system behavior in various regions of the predation probability P_p and the probability P_g at which juveniles grow into adults. Note how the parameter region where the infection is absent (because of predation) gets larger as P_g increases. See text for explanation. The remaining parameters are $P_c = 0.01$, $P_b = 0.02$, $P_K = 0.925$ and $P_a = 0.3$.

possess two bifurcations as P_g is varied. The first is related to the existence of a non-zero susceptible population, and the second to the appearance of the infected phase. On the other hand, if $P_p = 0$, these two transition points merge into a single one at $P_g = 0$. In order to better understand the existence of these bifurcations as P_g is varied, we approach the system through a mean field analysis in the next section.

3 Understanding the results from mean field considerations

An understanding of the simulations results reported above may be attempted through mean field considerations. A mean field (no space resolution) representation of the model in equations (1) above, equivalently in the simulations rules set out in Sec. 2, is

$$\begin{aligned}
\frac{d\mathcal{B}_i}{d\tau} &= -(\gamma + \delta)\mathcal{B}_i + \alpha\mathcal{B}_s\mathcal{A}_i + 2\alpha\mathcal{B}_i\mathcal{B}_s - \mathcal{B}_i(\mathcal{A} + \mathcal{B}), \\
\frac{d\mathcal{B}_s}{d\tau} &= -(\gamma + \delta)\mathcal{B}_s + \beta(\mathcal{A}_s + \mathcal{A}_i) - \alpha\mathcal{B}_s\mathcal{A}_i - 2\alpha\mathcal{B}_i\mathcal{B}_s - \mathcal{B}_s(\mathcal{A} + \mathcal{B}), \\
\frac{d\mathcal{A}_i}{d\tau} &= -\mathcal{A}_i + \alpha\mathcal{A}_s\mathcal{B}_i + \gamma\mathcal{B}_i - \mathcal{A}_i(\mathcal{A} + \mathcal{B}), \\
\frac{d\mathcal{A}_s}{d\tau} &= -\mathcal{A}_s - \alpha\mathcal{A}_s\mathcal{B}_i + \gamma\mathcal{B}_s - \mathcal{A}_s(\mathcal{A} + \mathcal{B}),
\end{aligned} \tag{2}$$

where $\tau = ct$. Each script character in (2) is dimensionless and denotes the ratio of the quantity described by the corresponding Roman character in (1) and cK . The other dimensionless quantities are the parameters $\gamma = g/c$, $\beta = b/c$, $\delta = c_B/c$ and $\alpha = Ka$. As explained elsewhere (Kenkre et al., 2005), we take the rate associated with the transfer of infection between two juveniles to be twice that between a juvenile and an adult. This is in keeping with similar considerations of the description of excitation capture and annihilation processes in molecular crystals (Kenkre and Reineker, 1982; Pope and Swenberg, 1999) and represents the situation when motion of the juveniles is slow with respect to the actual infection process.

The steady state solutions of the set of equations (2) can be found analytically in terms of the system parameters by noticing that the total adult and juvenile population evolves in time according to

$$\begin{aligned}
\frac{d\mathcal{B}}{d\tau} &= \beta\mathcal{A} - (\gamma + \delta)\mathcal{B} - \frac{\mathcal{B}(\mathcal{A} + \mathcal{B})}{cK}, \\
\frac{d\mathcal{A}}{d\tau} &= -\mathcal{A} + \gamma\mathcal{B} - \frac{\mathcal{A}(\mathcal{A} + \mathcal{B})}{cK}.
\end{aligned} \tag{3}$$

It is easy to see from Eq. (3) that the total mice population $\overline{\mathcal{A}} + \overline{\mathcal{B}}$ does not follow a logistic growth, contrary to what occurs in the original model (Abramson and Kenkre, 2002) for the spread of the Hantavirus. As a consequence, $\overline{\mathcal{A}} + \overline{\mathcal{B}}$ is not linearly proportional to β . It is straightforward to find from Eq. (3) the total population at steady state, i.e., the carrying capacity of the system normalized to cK . When $\beta < 1 + \delta/\gamma$, there is the trivial case $\overline{\mathcal{A}} + \overline{\mathcal{B}} = 0$, while, with $\beta > 1 + \delta/\gamma$, the normalized carrying capacity is given by

$$\overline{\mathcal{A}} + \overline{\mathcal{B}} = (\beta - 1 - \delta/\gamma) \frac{\gamma}{1 + \delta + \gamma} \frac{\sqrt{1 + 2\chi} - 1}{\chi}, \tag{4}$$

where $\chi = 2(\beta - 1 - \delta/\gamma)\gamma(1 + \gamma + \delta)^{-2}$. Limiting analysis of Eq. (4) shows that the carrying capacity increases linearly with β close to the bifurcation, and is proportional to $\sqrt{\beta}$ for $\beta \rightarrow \infty$.

A stability analysis shows that the bifurcation at $\beta = 1 + \delta/\gamma$ is transcritical. The interesting δ/γ dependence of this bifurcation can be explained as fol-

lows. If juveniles die too fast (large δ) or become adult too slowly (γ small), further generation of juveniles is prevented. Both these mechanisms act towards a reduction, and eventual disappearance, of the adult population. The disappearance of the adult population, in turn, can make the entire population collapse to zero at long times. The growth rate γ counteracts the effect of δ because the conversion of juveniles to adult status makes them resident and thereby inaccessible to predators in our model. This dependence on δ/γ is reflected also in the adult and juvenile population as can be seen from their values at steady state.

$$\begin{aligned}\bar{\mathcal{B}} &= \left[\frac{(\beta - 1 - \delta/\gamma)}{-1} \right] \gamma \frac{(\beta + \delta + \gamma) (\sqrt{1 + 2\chi} - 1) - \chi(\gamma + \delta + 1)}{\chi}, \\ \bar{\mathcal{A}} &= \left[\frac{(1 + \gamma)(\beta - 1 - \delta/\gamma)}{(1 + \gamma + \delta)(\beta + \delta - 1)} \right] \gamma \frac{1 + \chi(1 + \gamma + \delta)(1 + \gamma)^{-1} - \sqrt{1 + 2\chi}}{\chi}.\end{aligned}\quad (5)$$

In the limit $\delta \rightarrow 0$, Eq. (6) reduces to mean field results previously reported (Kenkre et al., 2005) in the absence of predators. Some additional algebra allows us to express the steady-state infected and susceptible populations in terms of $\bar{\mathcal{A}}$ and $\bar{\mathcal{B}}$. The phase with no infection is simply given by $\bar{\mathcal{B}}_i = 0 = \bar{\mathcal{A}}_i$, $\bar{\mathcal{B}}_s = \bar{\mathcal{B}}$, $\bar{\mathcal{A}}_s = \bar{\mathcal{A}}$, while the infected phase can be written as

$$\begin{aligned}\bar{\mathcal{B}}_i &= \frac{\sqrt{\mathcal{F}^2 + 8\mathcal{E}} - \mathcal{F}}{4\alpha}, & \bar{\mathcal{B}}_s &= \bar{\mathcal{B}} - \bar{\mathcal{B}}_i, \\ \bar{\mathcal{A}}_i &= \frac{\bar{\mathcal{B}}_i(\gamma + \alpha\bar{\mathcal{A}})}{\alpha\bar{\mathcal{B}}_i + 1 + \bar{\mathcal{A}} + \bar{\mathcal{B}}}, & \bar{\mathcal{A}}_s &= \bar{\mathcal{A}} - \bar{\mathcal{A}}_i,\end{aligned}\quad (6)$$

wherein $\mathcal{E} = \alpha\bar{\mathcal{B}}(\gamma + \alpha\bar{\mathcal{A}}) - [\gamma + \delta + \bar{\mathcal{A}} + \bar{\mathcal{B}}(1 - 2\alpha)](1 + \bar{\mathcal{A}} + \bar{\mathcal{B}})$ and $\mathcal{F} = 2(\gamma + 1) + \bar{\mathcal{A}}(3 + \alpha) + \bar{\mathcal{B}}(3 - 2\alpha)$. Similarly to the mean field analysis (Kenkre et al., 2005) of this model in the absence of predators, a stability analysis allows us to determine that infection exists only when the infection parameter is larger than a critical value, or similarly, when the environment parameter K is larger than the critical value:

$$K_c = \frac{\gamma + 2(1 + \bar{\mathcal{A}} + \bar{\mathcal{B}})}{2\alpha\bar{\mathcal{A}}} \left\{ \sqrt{1 + \frac{4\bar{\mathcal{A}}(\gamma + \delta + \bar{\mathcal{A}} + \bar{\mathcal{B}})(1 + \bar{\mathcal{A}} + \bar{\mathcal{B}})}{\bar{\mathcal{B}}[\gamma + 2(1 + \bar{\mathcal{A}} + \bar{\mathcal{B}})]^2}} - 1 \right\}.\quad (7)$$

The analytical derivation of the steady state mean field allows us to generate the phase plots of the system and compare them with those from the simulation. The $\delta - \gamma$ phase plane is presented in Fig. 4. It shows when infection is present and when a non-zero population exists. The straight line is $\delta = \gamma(\beta - 1)$ while the curve limiting the region of infection is obtained by

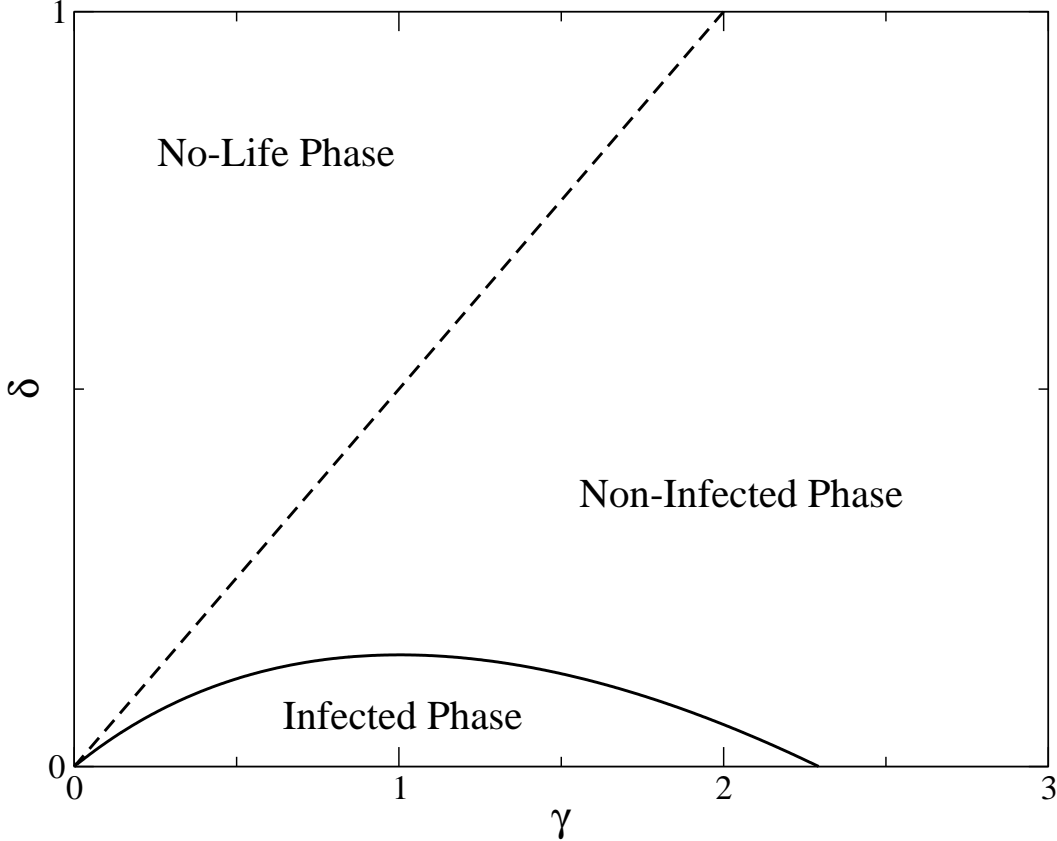


Fig. 4. $\delta - \gamma$ phase plot for the mean field equations (2). The straight line is given by $\delta = \gamma(\beta - 1)$ while the curve separating the region of infection from the region without infection is obtained by finding the implicit function defined by setting the quantity $\mathcal{E}(\delta, \gamma)$ defined in the text equal to zero. Parameter β and a are chosen to be 1.5 and 5 (arbitrary units), respectively.

finding the implicitly defined function $\mathcal{E}(\delta, \gamma) = 0$. The reasons for the presence of a maximum in the $\mathcal{E}(\delta, \gamma) = 0$ curve can be explained as follows. When $\gamma = 0$, juveniles cannot become adults and new juveniles cannot be born. The system is thus driven to extinction because of predation and competition. Alternatively, it is easy to see that the only steady state solutions in Eq. (3), when $\gamma = 0$, are the trivial case $\mathcal{A} = \mathcal{B} = 0$. An increase in γ from zero helps infection since adults are necessary to generate more juveniles. The latter are primarily responsible for spreading the infection. A non-zero γ may thus give rise to infection if δ is sufficiently small as can be seen by the sublinear increase of the $\mathcal{E}(\delta, \gamma) = 0$ curve in Fig. 4. However, beyond a certain value of γ infection is hampered: juveniles are converted too fast into adults and do not have the time to meet other individuals and spread the infection. This effect is the more pronounced the larger the predator pressure. This explains the curvature of the $\mathcal{E}(\delta, \gamma) = 0$ curve beyond its maximum. Simulations do not possess this transition since clusters of adults are generated by increasing P_g in the system. Infection is actually helped by increasing P_g beyond a certain value.

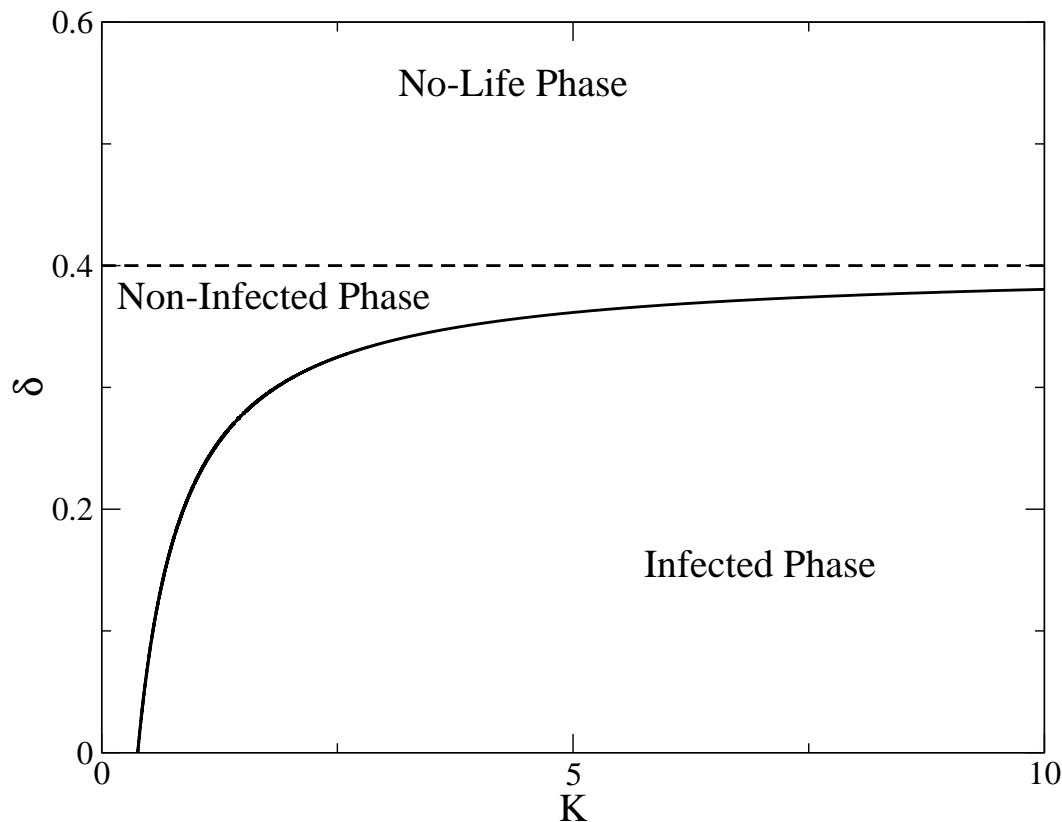


Fig. 5. Mean field phase plot in the $\delta - K$ plane. The horizontal line is given by $\delta = \gamma(\beta - 1)$ while the curve separating the infected from the susceptible phase is simply the graph of Eq. (7). The other parameters are: $\beta = 1.4$, $\gamma = 1$ and $a = 10$ in arbitrary units.

Differences between the simulation and the mean field results are also observed when comparing the $\delta - K$ phase plot in Fig. 5 with the corresponding simulation phase plot in Fig. 2. Qualitatively different curves separate the regions of non-zero steady state populations from regimes where no population persists at long times. In the mean field the no-life phase is independent of K while it strongly depends on P_K in Fig. 2. This difference is understandable since in the simulation the death by predators and the death by competition act together to drive the system to extinction, while in the mean field, only if $\delta > \gamma(\beta - 1)$ or if $K = 0$, the steady state population is zero. Such differences in extinction behaviour in the predictions of mean field versus more accurate descriptions can arise because discreteness and finiteness of numbers of mice are neglected in the mean field analysis. Comments on these differences have appeared in earlier literature (Aguirre et al., 2002; Escudero et al., 2004).

The other important qualitative difference between the two levels of description of our model can be seen by noticing that

$$K_c \approx \frac{1}{a} \frac{f(\beta, \gamma)}{(\beta - 1)\gamma - \delta},$$

as δ approaches $\gamma(\beta - 1)$ from below. Here, $f(\beta, \gamma) = (2\gamma)^{-1}(1 + \gamma)(2 + \gamma)(1 + \beta\gamma) \left\{ [1 + 4\beta\gamma^2/(2 + \gamma)^2]^{1/2} - 1 \right\}$. This means that the line that separates the infected from the susceptible phase in Fig. 5 converges at large K to the line that separates the susceptible phase from the phase with zero population. Therefore, as the population grows (linearly) with K , an infected phase will always appear beyond a certain value of the environment parameter. In the mean field a region in parameter space where the population, upon increase of K , does not become infected exists only in the trivial case corresponding to $a = 0$.

4 Conclusions

The analysis of the effect of predators of juvenile rodents presented in this paper completes our preliminary studies of the so-called LS model of stationary adult rodents and itinerant juveniles introduced earlier (Kenkre et al., 2005). We have found that a non-infected phase emerges as a transcritical bifurcation as function of the predation ‘pressure’. The LS model owes its existence to a detailed study of field observations on rodents carried out recently (Giuggioli et al., 2005; Abramson et al., 2005) on *Zygodontomys brevicauda* in Panama and on *Peromyscus maniculatus* (Stickel, 1968) in New Mexico. That study necessitated a generalization of a previous model (Abramson and Kenkre, 2002) into the LS model (Kenkre et al., 2005) to incorporate observed home ranges (Giuggioli et al., 2005).

A realistic modeling of the Hantavirus epidemic needs to represent the fact that an adult mouse is less prone to predation in comparison to a juvenile mouse. Familiarity of the area inside a home range provides a resident mouse with higher security and shelter from intruders, minimizing the chance of its being killed by predators. A non-trivial utilitarian consequence of our present analysis is the possibility of buffering and even eliminating infection without killing off the mouse population. Ongoing work in our group is focussed on kinetic level investigations as well as traveling wave studies in these systems.

Acknowledgements

We acknowledge helpful conversations with David MacInnis, Guillermo Abramson, Marcelo Kuperman, Terry Yates and Robert Parmenter. This work was supported in part by the NSF under grant no. INT-0336343, by NSF/NIH Ecology of Infectious Diseases under grant no. EF-0326757, and by DARPA under grant no. DARPA-N00014-03-1-0900. We acknowledge the Center for

High Performance Computing, UNM, for making available to us their computing resources.

References

- Aguirre, M.A., Abramson, G., Bishop, A.R., Kenkre, V.M., 2002. Simulations in the mathematical modeling of the spread of the Hantavirus. *Phys. Rev. E* 66, 041908-1-5.
- Abramson, G., Kenkre, V.M., 2002. Spatio-temporal patterns in the Hantavirus infection. *Phys. Rev. E* 66, 011912-1-5.
- Abramson, G., Kenkre, V.M., Yates, T.L., Parmenter, R.R., *Bull. Math. Biol.* **65**, 519 (2003).
- Abramson, G., Giuggioli, L., Kenkre, V.M., Dragoo, J., Parmenter, R.R., Parmenter, C.A., Yates, T.L., 2005. Diffusion and home range parameters for rodents: *Peromyscus Maniculatus* in New Mexico. *Ecol. Complexity*, in press.
- Buceta, J., Escudero, C., de la Rubia, F. J. and Lindenberg, K., 2004. Outbreaks of Hantavirus induced by seasonality. *Phys. Rev. E* 69, 021906-1-8.
- Escudero, C., Buceta, J., de la Rubia, F.J., Lindenberg, K., 2004. Effects of internal fluctuations on the spreading of Hantavirus. *Phys. Rev. E* 70, 061907-1-7.
- Giuggioli, L., Abramson, G., Kenkre, V.M., Suzán, G., Marcé, E., Yates, T.L., 2005. Diffusion and home range parameters from rodent population measurements in Panama. *Bull. Math. Biol.* 67, 1135-1149.
- Giuggioli, L., Abramson, G., Kenkre, V.M., Parmenter, R.R., Yates, T.L., 2005. *J. Theor. Biol.* in press.
- Kenkre, V.M., Reineker, P., 1982. *Exciton Dynamics in Molecular Crystals and Aggregates*. Springer-Verlag, Berlin.
- Kenkre, V.M., 2003. Memory formalism, nonlinear techniques, and kinetic equation approaches. In: Kenkre, V. M., Lindenberg, K. (Eds.), *Modern Challenges in Statistical Mechanics: Patterns, Noise, and the Interplay of Nonlinearity and Complexity*, AIP Proc. vol. 658, Melville, NY, pp. 63-102.
- Kenkre, V.M., 2005. Statistical mechanical considerations in the theory of epidemics. *Physica A* 356, 121-126.
- Kenkre, V.M., Giuggioli, L., Abramson, G., Camelo-Neto, G., 2005. Theory of Hantavirus infection spread incorporating localized adult and itinerant juvenile mice. *Phys. Rev. E* submitted.
- Mills, J. N., Ksiazek, T. G., Peters, C. J. and Childs, J. E. (1999). Long-term studies of hantavirus reservoir populations in the southwestern United States, a synthesis. *Emerging Infectious Diseases* 5, 135-142.
- Pope, M., Swenberg, C.E., 1999. *Electronic Processes in Organic Crystals and Polymers*. Oxford, New York.
- King, J.A., (editor), 1968. *Biology of Peromyscus (Rodentia)*. Special Publication No. 2, The American Society of Mammalogists, Stillwater, OK.

Yates, T. L., Mills, J. N., Parmenter, C. A., Ksiazek, T. G., Parmenter, R. R., Vande Castle, J. R., Calisher, C. H., Nichol, S. T., Abbott, K. D., Young, J. C., Morrison, M. L., Beaty, B. J., Dunnun, J. L., Baker, R. J., Salazar-Bravo, J., Peters, C. J., 2002. The ecology and evolutionary history of an emergent disease, Hantavirus Pulmonary Syndrome. *Bioscience* 52, 989-998.